Combination of musculoskeletal and wear models to investigate the effect of daily living activities on wear of hip prostheses

Authors

Lorenza Mattei, Matilde Tomasi, Alessio Artoni, Enrico Ciulli, Francesca Di Puccio

Abstract

Numerical wear predictions are gaining increasing interest in many engineering applications, as they allow to simulate complex operative conditions not easily replicable in the laboratory. As far as hip prostheses are concerned, most of the wear models in the literature are based on the simulation of gait (recommended also in experimental wear tests), since gait is considered the most frequent and important motor task to recover after arthroplasty. However, since joint prostheses have been increasingly implanted in younger people, high loads and potentially severe conditions, e.g. due to sporting activities, should also be considered for a more reliable wear assessment of these implants.

In this study, we propose a profitable combination of musculoskeletal and analytical wear modelling for the prediction of wear caused by common daily activities in metal-on-plastic hip arthroplasties. Several motion analysis data available in the literature (walking, fast walking, lunge, squat, stair negotiation) were selected and the effects of such motor tasks on prosthesis wear were investigated, both separately and in combination. Additionally, for comparative purposes, wear prediction for simplified gait conditions prescribed by the ISO 14242 standard, were also considered. Results suggest that this latter case produces lower wear depth and volume with respect to a relatively demanding combination of the selected daily activities. The preliminary results of the present study represent a first step towards the auspicious goal of validating the proposed procedure for *in silico* trials of hip arthroplasties.

1 Introduction

Numerical wear predictions are gaining increasing interest in many engineering applications, from gears to biomedical devices, as they can provide cheaper and faster indications with respect to experimental tests. Another advantage, particularly attractive in the Biotribology of joint prostheses, is the possibility of easily simulating complex and diverse physiological scenarios, and thus of predicting wear in *in vivo* conditions.

As far as hip arthroplasties (HAs) are concerned, preclinical trials are based on experimental wear tests performed in hip joint simulators, which reproduce loading and kinematics conditions that are very simplified with respect to the *in vivo* ones. For instance, the regulatory preclinical testing standard ISO 14242-1 prescribes a simplified gait cycle, with a vertical load and sinusoidal waveforms for the rotation angles. As discussed in [1,2], current preclinical tests of HAs are able to capture neither the variation in loads and kinematics of daily activities, nor the one among patients, although this is becoming more and more important: indeed, hip arthroplasty is performed in increasingly younger patients [3], whose implants can be subjected to high loads, for example during sporting activities. Though the literature counts many studies on experimental wear tests, most of them are based on simplified walking conditions and only rarely different motor tasks, such as jogging, are considered [4,5].

On the other hand, numerical wear models of hip joint prostheses are mostly used to simulate wear tests, as reviewed in [6,7]. Only in few cases, *in vivo* loading conditions from instrumented HAs [5,6] and kinematics from motion analysis recordings [8,9] are simulated. One example by the present authors is described in [10,11]; more recently, studies [12–14] compare wear predictions caused by several daily activities. All these investigations demonstrate how sensitive wear is to the loading conditions, and they suggest that using ISO 14242 for wear assessment can underestimate what happens, particularly in younger and more physically demanding patients. Thus, numerical wear predictions have a great potential, e.g., in *in silico* clinical trials, that is not fully exploited yet.

As reviewed in [6,7], most wear models are based on the assumption of dry contact between the articular surfaces and on the implementation of the Archard wear law in its original or other revised forms, e.g. for modelling the cross-shearing of ultra-high-molecular-weight polyethylene (UHMWPE). Indeed, the lubrication promoted by the synovial fluid even after arthroplasty is only rarely modelled. More frequently, it is taken into account through a wear coefficient estimated from experimental tests where lubrication is present. Only a couple of recent studies propose advanced wear models for metal-on-plastic (MoP) hip implants based on mixed lubrication modelling [12,15]. In particular, in [12] the real surface topography is considered and the surface evolution is predicted for long term wear, whilst in [15], geometry modifications are not modelled and wear is predicted for a single gait cycle. Although both these models are certainly more complete than the ones based on dry contact, they predict very similar wear rates, with percentage differences lower than 5% [12,16]. Thus, the development and application of simplified models without lubrication can be justified, particularly for obtaining indications in short computational times.

The reliability of wear predictions requires, first of all, the "correct" input data, including kinematics, joint reaction forces and wear coefficients. However, such inputs are difficult to estimate. On the one hand, reliable *in vivo* joint loads can be obtained by instrumented implants, an invasive and not so common procedure. In the literature, such loads are often reported without specifying the corresponding joints kinematics. On the other hand, the estimation of the wear coefficient requires a comparison between numerical and experimental wear volumes obtained from wear tests that simulate the same tribological scenario [17,18]. Unfortunately, as already mentioned, most of the daily activities have never been tested experimentally or wear coefficient is not reported or assessable by published data [5]. For instance, wear models of [12,13] assume constant wear coefficients, equal for all the activities, and equal for head and cup in case of metal-on-metal couples [13], which are both limiting assumptions [4,18].

Regarding the first issue, musculoskeletal (MSK) modelling represents a valuable option to estimate joint loads starting from non-invasive motion analysis [1,19–21]. This approach is adopted in the present study with the aim to define a general procedure for wear prediction of MoP HAs, which could be used in *in silico* pre-clinical trials, investigating the effect of several daily living activities on wear. Motion analysis data collected for a subject with a right HA during walking, fast walking, lunge, squat and stair negotiation from the dataset provided by Lunn et al. [22–24] are given as input to an MSK model developed in OpenSim to estimate both joint angles and joint reaction forces. These are then passed to the wear model of a 28 mm MoP implant, developed in Matlab®, for the prediction of both volumetric and linear wear. The damage of each single activity and of a combination of them are estimated and compared to the wear rates caused by the simplified gait conditions prescribed by ISO 14242.

The novelty of this study consists in the combination of the MSK and analytical wear models to investigate daily wear caused by common physical activities during the running in phase. The strength of the analytical approach is in its parametric formulation and its low computational cost, both fundamental requirements to perform an extensive campaign of *in silico* pre-clinical trials. Moreover, the wear model is a revision of the one presented in [10] and presents an improved contact analysis according to Bartel's theory [17,25].

2 Methods

A flow chart of the *in silico* procedure proposed to predict wear is given in Figure 1. Motion analysis data collected for a subject with a right HA are given as input to an MSK model in OpenSim in order to compute hip joint angles and loads. The latter, together with the implant characteristics, are used in the wear model to predict how the plastic surface of the cup is damaged. More details on MSK and wear modelling are provided in the following sections.

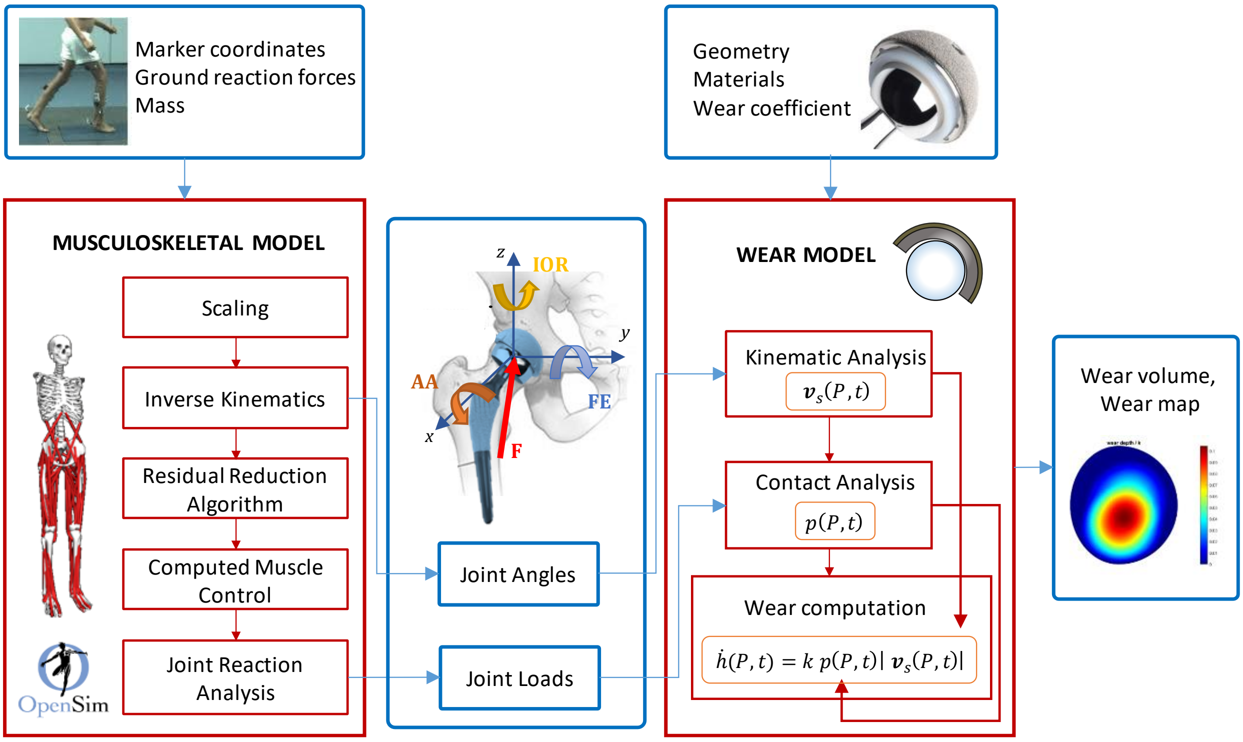

Figure 1 General flow chart of the MSK-wear modelling procedure.

2.1 MSK modelling

2.1.1 Dataset

Experimental motion analysis data were taken from the dataset provided by Lunn et al. within the LLJ European project [22–24], where a total of 140 patients with total hip replacement (THR) undertook motion capture while performing different activities of daily living. The present study is based on a single subject (LLJ_140) whose characteristics are shown in Table 1.

Subject	Gender	Age	Weight (kg)	Height (cm)	Operated limb	Years post operation
LLJ_140	M	65	64	168	Right	1

Table 1: Characteristics of the subject LLJ_140 analysed in the present study.

Within the present work, three locomotor tasks (i.e., normal and fast walking, and stairs negotiation) and two non-locomotor tasks (i.e., squat and lunge) were investigated. Indeed, walking is considered the most frequently performed activity of daily living, followed by stair negotiation. Also squatting, or a variation of squat, is performed daily, as for example while toileting or sitting and rising from a chair. Lunge resembles other motor tasks such as overcoming obstacles or performing some sport gestures like during tennis. Additional details on how these activities have been performed can be found in [23]. For the purpose of the present study, a single representative trial for each task has been considered.

Experimental data were lowpass-filtered to reduce noise associated with the acquisition process. In particular, a Butterworth filter at 6 Hz and 15 Hz was used for kinematic and kinetic data, respectively.

2.1.2 MSK model and simulations

MSK modelling (Figure 1) was performed using the open-source platform OpenSim [26], differently from [22,23,27], where AnyBody® was preferred. In particular, a 23 degree-of-freedom (dof) musculoskeletal model (i.e., gait2392), provided with 92 musculotendon actuators [28,29], was adopted and properly scaled to match the subject's anthropometric measures. Such model comprises the lower limbs and trunk, while the inertial properties of the arms are lumped in with those of the torso. The 23 dofs are distributed as follows: 6 dofs for pelvic translations and rotations with respect to the ground, 3 dofs (ball-and-socket joint) for the lumbar and hip joints, 1 dof at each knee and ankle joint, and 1 dof for the subtalar joint. Ninety-two Hill-type contractile elements in series with tendons actuate the model: 43 for each leg and 6 for the torso.

Inverse kinematics [30] was performed on the scaled model in order to obtain the joint angles that best fit the experimental marker trajectories. Both scaling and inverse kinematics are considered accurate enough if the RMS and maximum errors on marker positions were below 1 cm and 2 cm, respectively.

Dynamic consistency between the model kinematics, inertial properties and the measured ground reaction forces was improved through the Residual Reduction Algorithm (RRA) [31]. RRA produces an adjusted kinematics and a model with adjusted inertial properties, which were then used for the subsequent simulations. Muscle activations that drive the model towards the desired kinematics were estimated through the Computed Muscle Control (CMC) algorithm [32]: it combines a proportional derivative control with static optimization, taking into account both the muscle dynamics and the force-length-velocity relationship of muscles. In particular, the static optimization step redistributes net joint torques among muscles while minimizing the sum of squared muscle activations. Muscle forces were then calculated through the musculotendon actuator model and its parameters. Finally, the estimated muscle forces were input to the Joint Reaction Analysis (JRA) [33] algorithm to estimate the loads at the hip joint during movement. JRA proceeds recursively, starting from the most distal body, and solves the equations of motion at each segment, given the kinematics, inertial properties, and muscle forces. Since the hip joint was modelled as an ideal spherical joint with no friction, only the three force components were nonzero. Dynamic simulations were deemed successful if residual forces and torques, as well as reserve actuators, were within the bounds specified by the OpenSim guidelines and by [25], and kinematic errors were within 2 cm for translations and 2° for rotations.

2.2 Wear modelling

2.2.1 Wear model

Wear modelling was based on an analytical approach which allows very rapid simulations of the surface damage during the running-in phase [34]. The wear model presented in [10] for MoP HAs was revised and improved in terms of contact analysis. This section describes the model briefly, while further details can be found in [10,34].

The model is based on the main assumptions that the wear affects only the plastic cup, the geometrical variations caused by the material loss are negligible and do not affect contact mechanics, and contact is frictionless since the wear coefficient is lower than 0.065 [10,34].

Experimental investigations have demonstrated the complex anisotropic wear behaviour of UHMWPE in a multidirectional sliding condition, the so-called cross-shearing phenomenon. However, the debate on the validity of the specific wear laws and wear coefficient expression is still an open issue [10]. Consequently, in this study the classic Archard wear law with a constant wear coefficient k was assumed and implemented in local and instantaneous form as follows:

$$\dot{h}(P,t) = k\, p(P,t) |\, \boldsymbol{v}_s(P,t)| \quad (1)$$

stating that the linear wear rate $\dot{h}$ at a point P on the cup surface, at a given time t, is proportional to the contact pressure $p(P,t)$ and to the magnitude of the sliding velocity $\boldsymbol{v}_s(P,t)$.

As represented in Figure 1, the model takes as input the implant characteristics (geometry and material properties), wear coefficient, loading and kinematic boundary conditions (computed by the MSK model), and it predicts the implant wear through the following steps:

i) Contact analysis; the nominal contact point on the cup surface, Q, is first identified by considering its alignment with the cup and head centres in the direction of the joint load (see Figure 2(a)). Whilst in [10] the contact pressure distribution was estimated using data from finite element analyses, Bartel's formulas are adopted here, in much the same way as was done for the wear model of shoulder arthroplasty in [17]. It is worth reminding that they are based on the hypothesis of a rigid head in contact with a compliant (linear elastic) cup, with a finite thickness, externally constrained to a rigid backing. A comparison between the finite element results and Bartel's formula showed a very good agreement (maximum pressure error lower than 2% [17]) when the contact area did not reach the cup edge. This modification of the model has two advantages: it allows a purely analytical approach, and the model results parametric with respect to geometrical and material properties of the implant.

ii) Kinematic analysis; the sliding velocity is computed studying the relative rigid motion between the head and the cup.

iii) Wear computation; linear and volumetric wear are evaluated by integration:

$$h(P) = \int_0^T \dot{h}(P,t)\,dt \quad (2)$$

$$V = \int_A h(P)\,dA \quad (3)$$

Differently from [10,34], the model was implemented in Matlab®. Figure 2 gives some details on the model showing (a) the ball-and-socket geometry, (b) the coordinate frame attached to the cup, and (c) the application of boundary conditions. In particular, the joint load **F** is applied to the cup, considered fixed, while the head/cup relative motion is applied to the head through the rotation sequence flexion/extension (FE), ab/adduction (AA), and inward/outward rotation (IOR).

The cup surface was discretized into 4141 points and the loading history into 50 frames. Each simulation required only a few seconds.

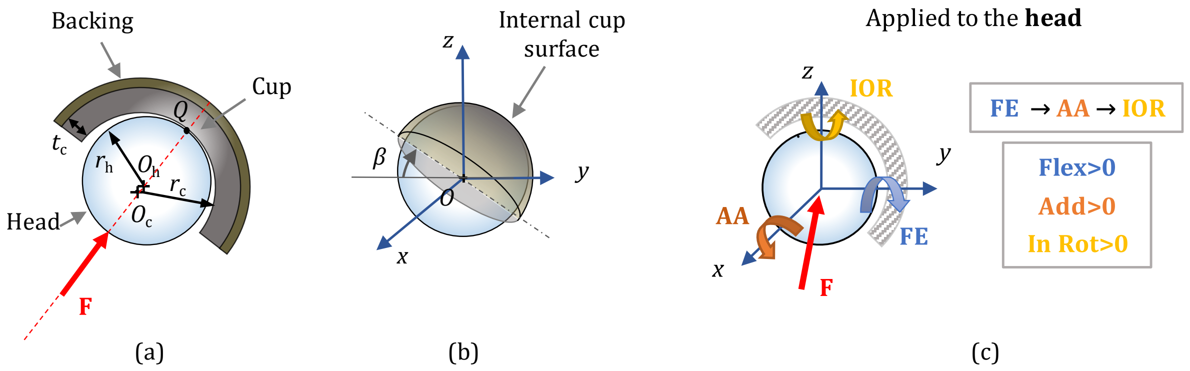

Figure 2 Wear model geometry (a,b), coordinate frame attached to the cup (b) and application of rotations and load to the head and cup, respectively (c). The nominal contact point Q in shown in Figure 2(a).

2.2.2 Implant type

As a case study, a 28-mm MoP HA was considered. Since the dataset from [22–24] does not provide any information on the subject's implant type, we considered the same case study as in [10], so that results are comparable with the literature. The following data were assumed: head radius r_h=14 mm, cup radius r_c=14.08 mm (radial mismatch=0.08 mm), liner thickness t_c=8 mm, cup inclination β=35°; elastic modulus E and Poisson's ratio ν of the head and cup equal to E_h=210 GPa, ν_h=0.3 and E_c=0.5 GPa, ν_c=0.4, respectively. The traditional non-cross-linked UHMWPE was considered (i.e., irradiation dose equal to 0 MRad) and a constant wear coefficient k =1.066 10^{-6} mm^3/(Nm) [35] was assumed for all the activities since no specific k values are available in the literature.

2.2.3 Wear simulations

Wear simulations were performed both for each single activity analysed by the MSK model (i.e., gait, fast walking, squat, stairs up, stairs down, lunge) and for a combination of such daily activities. Though some studies describe the type [36] or the frequency [37] of daily activities, specific data for all the activities considered in the present study are not available. Combining data from current literature [5,14], the following numbers of task executions over 12 hours (i.e., cycles) were estimated and simulated to provide an estimate of daily wear: 1818 cycles of normal gait (40% of all 4545 cycles), 182 cycles of fast walking (4%), 1091 cycles of stair negotiation (24%, namely 12% stairs up and 12% stairs down), 1090 cycles of squatting (24%, representative of a 12% chair sitting and a 12% chair rising), and 364 cycles of lunges (8%). This scenario is indeed a relatively demanding one in terms of wear damage, and it was selected to be representative of a physically active subject.

Furthermore, the simplified gait conditions (hip load and angles) reported in the ISO 14242 standard for *in vitro* wear tests (Figure 3) were used as input in wear simulations for comparative purposes. As already stressed, the representativeness of the ISO 14242 conditions for HA wear assessment is an open issue in biotribology.

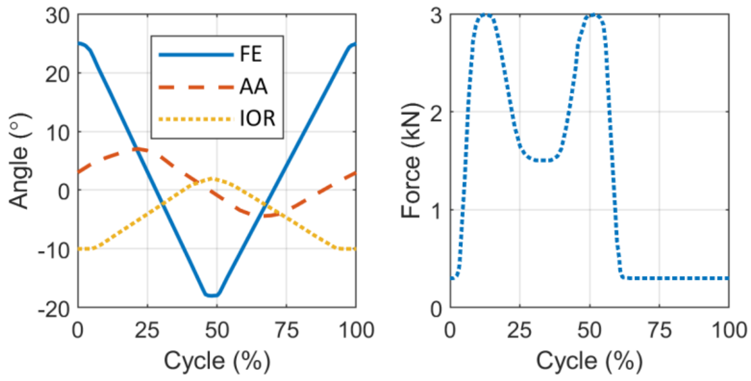

(a) (b)

Figure 3 Kinematic (a) and loading (b) conditions specified by ISO 14242. Force has only the vertical component.

3 Results

3.1 MSK model results: joint angles and loads

Figure 4 shows qualitative results from the OpenSim simulations for all the investigated motor tasks. In Figure 5 and Figure 6, quantitative results from the MSK simulations are represented in terms of hip kinematics and hip joint loads, expressed in the cup coordinate frame (Figure 2(b)). All simulation results have been presented for the operated limb. Trajectories of normal and fast walking are reported over a full gait cycle whereas those of squat, stairs, and lunge over their activity cycle.

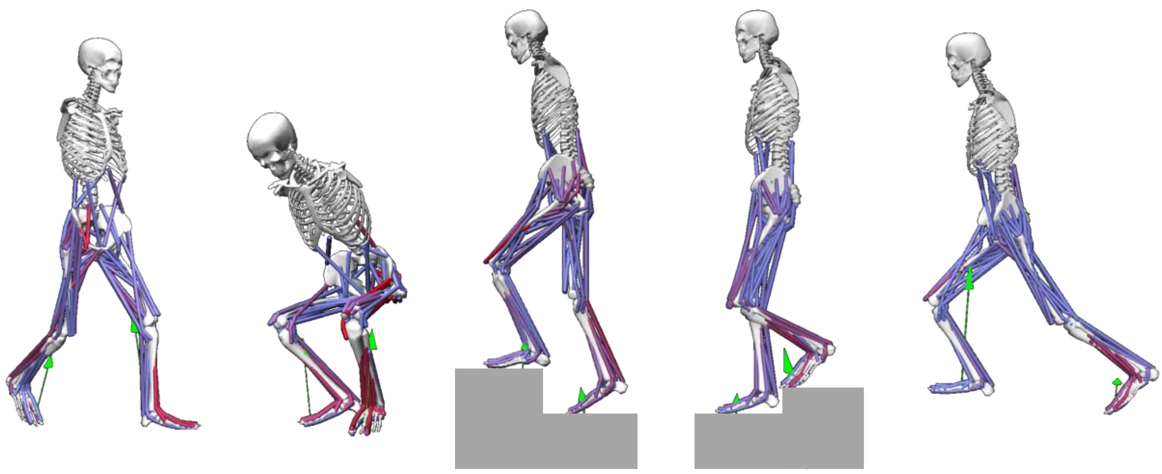

Figure 4 Snapshots from simulations in OpenSim for walking and fast walking, squat, stairs up, stairs down and lunge (green arrows: ground reaction force vectors).

3.1.1 Kinematics

Hip joint angles describe the orientation of the femur with respect to the pelvis. As already stated, the adopted rotation sequence is FE→AA→IOR. Flexion, adduction, and inward rotation are positive, while extension, abduction and external rotation are negative. As can be clearly seen from the plots in Figure 5, different tasks are associated with different hip kinematics, especially flexion, which is particularly high during squat and lunge. While walking and lunge show similar hip FE ranges of motion around 40°, squat exhibits a much larger ROM of about 100°.

3.1.2 Loads

Hip joint loads describe the forces acting at the femoro-acetabular level. In particular, Figure 6 shows the loads acting on the cup and expressed in the reference frame of the pelvis (i.e., fixed reference frame): F_x is the antero-posterior component, F_y is the medio-lateral component, F_z is the superior-inferior component. The comparison of individual force components across different activities reveals qualitatively different waveform patterns: in the two locomotor tasks, the vertical force F_z shows the typical pattern with two peaks, while it persists at high values in the two non-locomotor tasks for nearly all the duration of the activity. In general, predicted hip loads show good agreement with the overall trend and timing of the loads measured from the instrumented prostheses and reported in current literature (e.g., [7,8]), although an overall overestimation can be observed.

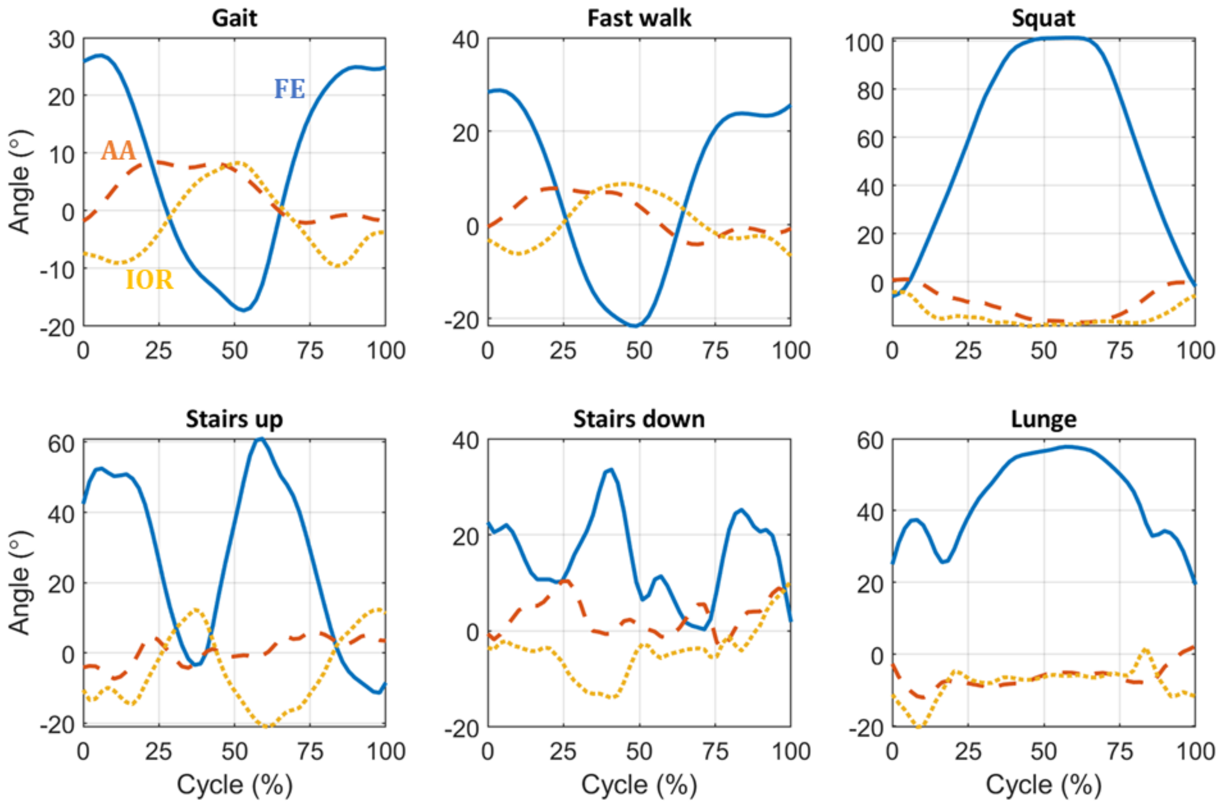

Figure 5 Hip joint angles for the analysed daily activities: walking, fast walking, squat, stairs up and down, and lunge. (Solid blue line: flexion-extension; dashed red line: adduction-abduction; dotted yellow line: internal-external rotation. Flexion, adduction, and inward rotation are positive, while extension, abduction and external rotation are negative, according to Fig. 2(c).)

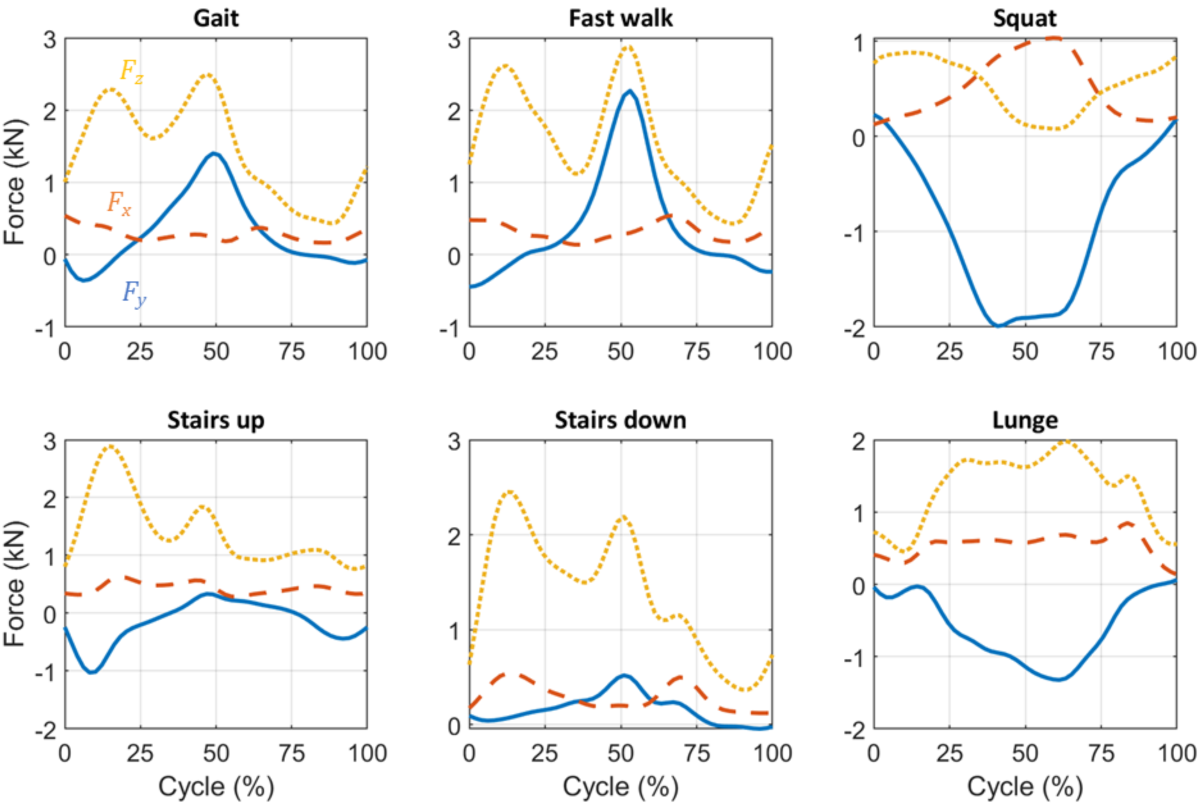

Figure 6 Hip joint loads for the analysed daily activities: walking, fast walking, squat, stairs up and down, and lunge. (Solid blue line: y or latero-medial force component; dashed orange line: x or postero-anterior force component; dotted yellow line: z or inferior-superior force component, according to Figure 2(c).)

3.2 Wear predictions

The trajectories of the nominal contact point Q and the wear maps predicted for each daily activity are shown on the left and right of Figure 7, respectively. Moreover, to ease the comparison, wear maps are represented both within their own minimum and maximum values (central column) and in the same range (right column).

The trajectory of Q is rather peculiar for each task. The gait and fast walking conditions produce similar quite oval trajectories, at similar locations. On the other hand, the trajectory of Q is elongated in the anterior-posterior direction for the squat, while it is rather multidirectional for stair negotiation and lunge. It is worth noting that the distance travelled by Q during stair climbing is much longer than that during stair descending.

Wear occurs in the surface region around the trajectory of Q, as well shown by the comparison between the left vs right columns of Figure 7. According to the shapes of the trajectories of Q, wear maps were almost circular for all the activities except for squat, which generated a stretched worn region in the anterior-posterior direction (Figure 7). In all cases, the maximum wear depth h_{max} was approximately located at the centre of the worn region.

The comparison of wear maps plotted with the same scale clearly shows that the wear rate is affected by the loading and kinematic conditions, and thus varies with the daily activity. It can be observed that the wear maps of the locomotor tasks were qualitatively similar, but quantitatively different. Stair negotiation was demonstrated to be much more demanding than gait and fast walking, particularly in stair climbing. The maximum wear depth per cycle was predicted to be in the range 0.115–0.275 × 10^{-6} mm, as summarized in the histogram of Figure 8(a), with the minimum and maximum values occurring for gait and stairs up, respectively. Gait, fast walking, squat, and lunge yielded very similar values for h_{max}.

Wear volume per cycle was much more sensitive to daily activities than maximum linear wear, although they are in agreement (obviously, wear volume depends on both linear wear and the worn area). The histogram in Figure (b) shows that volume predictions were in the range 14.17–31.56 × 10^{-6} mm^3. The lowest mass loss was predicted for lunges, while the highest for stair climbing, more than doubled in value. Walking speed was shown to affect wear volume: fast walking caused an increment in wear volume of about 40% compared to normal gait. Similar values around 21 × 10^{-6} mm^3 were predicted for squat and stairs down.

Regarding wear prediction for squat, a comment is necessary. As a matter of fact, the contact area extends up to the cup edge during squat execution: Bartel's formulas have limited validity when contact occurs around an edge, thus they should be regarded as a first approximation.

The *in vitro* simplified gait conditions prescribed by ISO 14242 to test wear of HAs were also used as input to evaluate differences in wear predictions both compared to *in vivo* gait and daily activities. Results are depicted in Figure . Wear predictions for *in vivo* and *in vitro* gait conditions were very similar. Wear maps were comparable both in shape and values, with values of maximum wear depth and wear volumes of 0.115 vs 0.134 × 10^{-6} mm and 14.42 vs 14.37 × 10^{-6} mm^3, respectively. It should be highlighted that *in vitro* conditions overestimated h_{max} (9%), but not wear volumes, probably because of the higher load level and the simplified kinematics (e.g., shorter sliding distances) considered by ISO.

The estimation of daily wear obtained considering the combination of all activities according to their daily frequencies (for a total of 4545 cycles as described in section 2.2.3) is shown in Figure 8 in terms of wear depth distribution, with a maximum depth value of 5.81 × 10^{-4} mm and a wear volume of 9.00 × 10^{-4} mm^3. On the other side, the application of the ISO standard for the same number of cycles produced a maximum wear depth of 6.09 × 10^{-4} mm and a wear volume of 6.5 × 10^{-4} mm^3. Thus, while h_{max} values are similar, the wear volume according to ISO conditions underestimated the one due to a task combination of about 40%. This suggests that such standard may not provide accurate predictions since *in vivo* conditions are more physically demanding than normal gait.

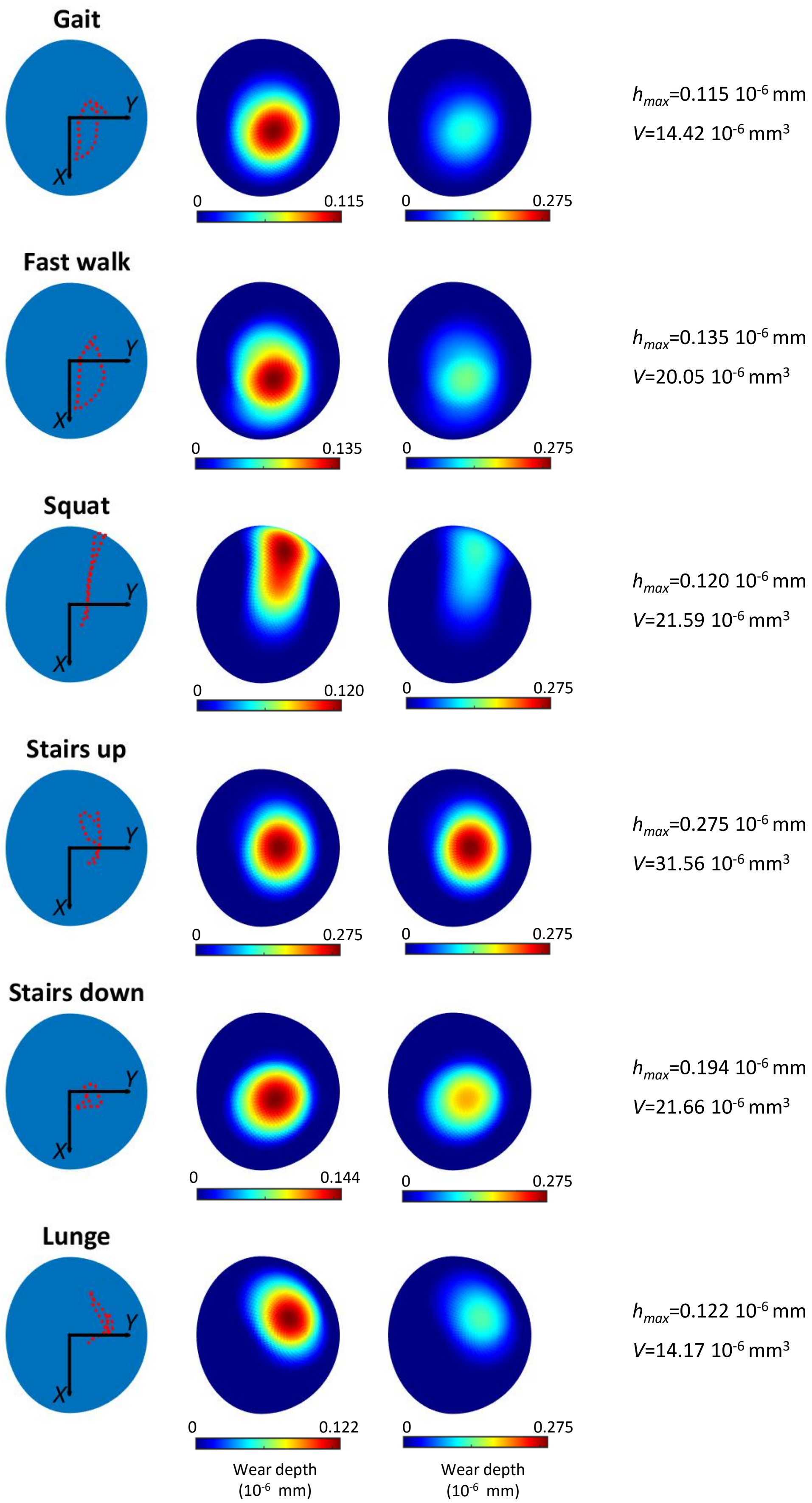

Figure 7 Trajectories of the nominal contact point Q (left column) and wear maps for one cycle of each activity, represented within its own minimum and maximum values (central column) and over the same range (right column, for ease of comparison).

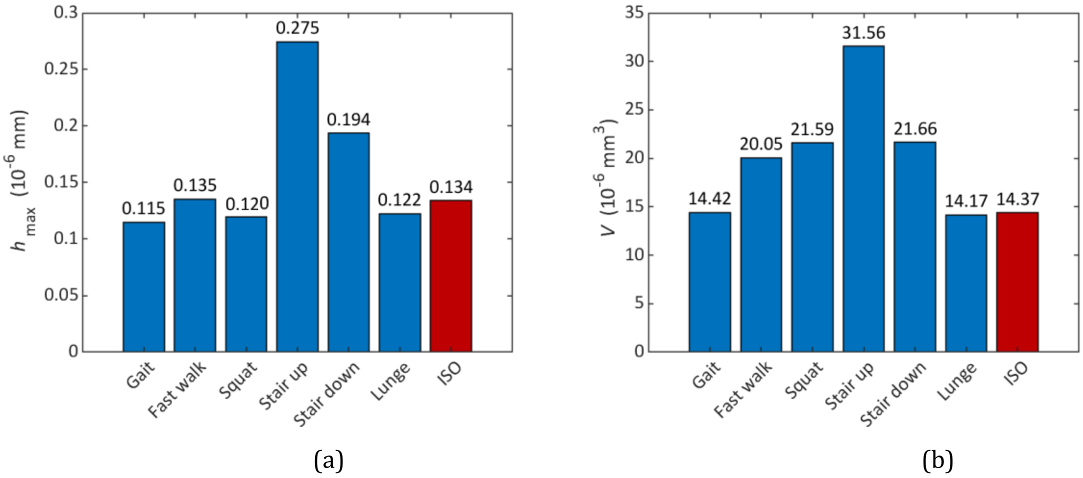

Figure 8 Maximum wear depths (a) and wear volumes (b) predicted for one cycle of each activity and using the ISO 14242 boundary conditions.

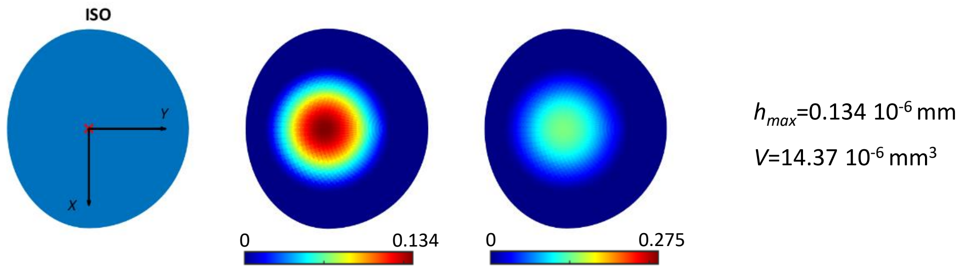

Figure 9 Trajectories of the nominal contact point (left column) and wear maps for one cycle of ISO 14242 conditions, represented within its own minimum and maximum values (central column) and over the same range as Figure 7 (right column, for ease of comparison).

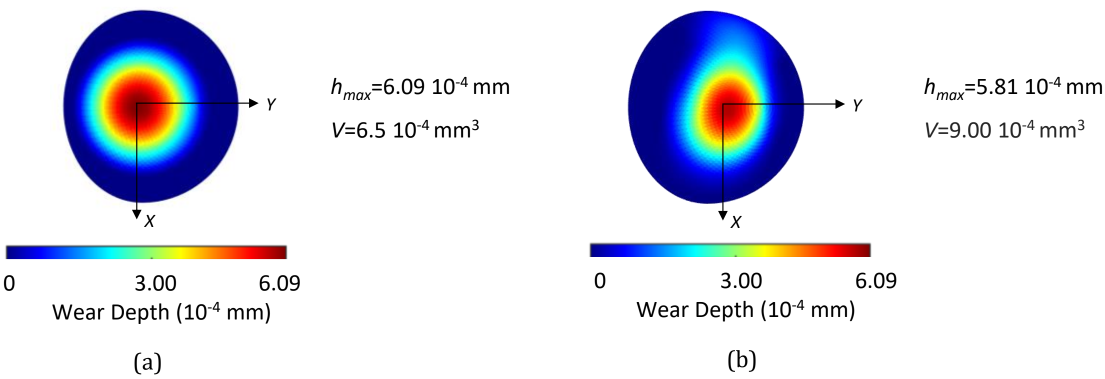

Figure 8 Daily wear map and volume predicted under conditions specified by ISO 14242 (a) and caused by the combination of all daily activities (b) (for a total of 4545 cycles).

4 Discussion

The present study combines MSK modelling with wear simulations to investigate the deterioration of hip joint prostheses during daily living activities. Limitations of the obtained results depend on both the adopted approaches.

4.1 MSK model limitations

MSK modelling was used to estimate hip joint kinematics and reaction forces. Even though the obtained hip joint loads are comparable to those reported in similar studies (e.g., [19,23,27,38]), they typically overestimate those measured by instrumented prostheses and reported in public databases (e.g., [8,9]). This may be due to the several limitations affecting MSK models in addition to uncertainties due to experimental data acquisition (e.g. soft tissue artefacts)[39].

First of all, in order to define a general procedure, we simply scaled the MSK Gait2392 model available in OpenSim, without performing a patient-specific adaptation of the musculoskeletal system, since this could be time consuming and not feasible with a large number of cases as in clinical practice. Similarly, several parameters defining the musculotendon architecture (e.g., optimal fibre length, tendon slack length, etc.) are not subject-specific: indeed, in the pre-defined OpenSim model Gait2392, they were derived from published cadaver studies. These simplifications do not allow to accurately reproduce both the skeletal and the musculotendon geometries, which are known to affect the estimation of joint loads [40–42].

A second issue concerns the Computed Muscle Control algorithm used to estimate muscle activations. CMC relies on a recruitment criterion that minimizes the sum of squared activations. Though this is in agreement with most studies in this field, other criteria could be used that may be more reliable for the specific patient/task. But this is another research topic in biomechanics and neuromuscular control.

Lastly, the absence of recorded electromyographic signals in the adopted motion analysis dataset did not allow to validate the estimated muscle activations, hence muscle forces, which are known to be a major contributor to joint loads.

4.2 Wear modelling limitations

As far as wear simulations are concerned, the adopted wear model was derived from [10] and improved in terms of the contact analysis equations, implementing Bartel's formulas for MoP implants. The model was validated for ISO 14242 conditions, providing wear rates in good agreement with a previous study for the same implant type (both geometry and material properties) [10]. Results were compared also to other numerical and experimental literature studies, where similar (but not equal) conditions were simulated, that is 28 mm MoP implants under simplified gait conditions (i.e., hip simulator conditions). Quite often, some important details of the model or of the wear tests are not described, thus the comparison can be only qualitative. For instance, *in silico* wear models developed by a research group from the University of Leeds [43–45] predicted volumetric wear rates in the ranges 13-27 mm^3/Mc, in agreement with the 14 mm^3/Mc of the present study. On the other hand, our model overestimates the linear wear, which is about 0.134 vs 0.035-0.07 mm/Mc from the literature, probably because of the different wear law adopted.

In the study [46] by Kaddick and Wimmer, 28 mm MoP hip implants (0 Mrad) were tested *in vitro* under ISO 14242 conditions (clearance not specified) reporting wear rates in good agreement with the present ones, i.e. 22.7 mm^3/Mc and about 0.1 mm/Mc. The higher volumetric wear rate might be due to the value of the clearance, which greatly influences the lubrication regime, as well as to the geometry changes due to wear not modelled in our study. The wear map measured at 5 Mc presented “a double peak”, i.e. two points with similar maximum wear depths, differently from our map with a “single peak”. This might be caused by surface evolution due to wear and not considered in the present model. However, our wear map is validated by other, more recent studies, such as [43,47,48].

Finally, several limitations should be stressed. Firstly, as already mentioned, this type of model does not include lubrication, considered e.g. in [12,15], but it takes it into account indirectly through the wear coefficient k in eq.(1). The value of this coefficient is usually considered constant through the wear process, assuming quasi-stationary conditions. Actually, the described activities represent transient conditions and also the geometry varies with time as a consequence of wear. This is probably one of the most critical issues, but a variable k is not defined in the literature, nor in laboratory conditions. Another point could be the choice of the wear law: we decided to use the simple Archard law, instead of more complex laws including cross shear, because the focus was on the simulated activity and we did not want to include further complications already discussed in a previous paper [10]. Again, for simplicity, we neglected the effect of time, i.e. creep or bedding in, that could be added in future developments.

4.3 Wear predictions

The wear model was firstly applied to estimate and compare wear caused by common daily activities. Similar circular wear maps were obtained for the selected locomotor tasks, though with different wear rates. Indeed, linear wear and even more volumetric wear proved to be sensitive to the loading conditions. Stair climbing turned out to be the more demanding motor task, with doubled wear rate compared to the normal gait. Also walking speed affects wear.

Secondly, daily wear caused by the combination of such activities was simulated, and limitations in wear predictions based on simplified gait conditions emerged. This is particularly true for more demanding motor tasks that deviate from simple walking.

Despite the above-mentioned limitations, results were in good agreement with the literature. To the best of the authors' knowledge, only two studies describe the effect of different daily activities on wear of MoP HAs [12,14]. They both considered a 32-mm HA and obtained loading and kinematic conditions by instrumented implants, though from different datasets ([8] for [14], and the less recent HIP98 [9] for [12]). Also in-vitro test conditions were considered (ISO 14242 [14] and HUT-3 [12]). A direct quantitative comparison of wear predictions is not possible since different implant geometries (radial clearance in addition to implant diameter) and wear coefficients were assumed. For instance, [12] adopted the same k value as in the present study, but the radial clearance is not specified, whilst [14] considered k as a function of contact pressure. However, similar conclusions were drawn. First of all, in full agreement with our study, stair climbing proved to be the more demanding activity, and [14] estimated for it almost double the wear rate in the HA compared to normal gait. However, in [14] the same wear rate for stairs up and down was predicted, but this was due to the assumption of having the same loading conditions (only different FE angles). On the other hand, [12] predicted a lower wear volume in stairs down than in stairs up, in agreement with our results. It should be noted that in this case, being the load level of the two conditions comparable, the different wear amounts are mainly caused by different kinematics. Interestingly, [14] predicted similar wear rate for squat and the ISO 14242 conditions, in agreement with the present study, confirming the need to consider activity-specific k values.

5 Conclusions

The main objective of the present study was to combine MSK modelling in OpenSim with wear simulations in Matlab® to predict the wear damage in hip joint prostheses during daily living activities. Additionally, we wanted to compare such wear prediction to the one obtained simulating the ISO 14242 conditions, which represent the current recommendations for *in vitro* wear tests.

The combination of the two approaches is strategic since MSK simulations can provide accurate hip joint kinematics along with joint loads, which only rarely are directly measurable, i.e. for the few patients with instrumented prostheses. Such data were input to a wear model implemented in Matlab® to predict volume loss and wear maps. The simple wear model was validated for some reference cases, and it represents a cheap and easy alternative to more complex finite element models. Since OpenSim can also be run through Matlab® scripts, this wear model could evolve into an OpenSim add-on in the future.

The proposed combined MSK-wear modelling procedure was applied to a single case study, and the obtained results are in good agreement with the literature, confirming the reliability of the adopted approach, despite some important limitations that will be addressed in the future. As next step of this research, the approach will be extended to larger patient and activity datasets, with the final goal of validating the procedure for *in silico* trials of HAs. Future research will also be devoted to improving the MSK model, especially for obtaining more accurate estimates of the loads acting at the acetabular level, as well as to improving the reliability of the wear model through the estimation of activity-specific k values or implementing more complex wear laws.

6 Acknowledgement

The authors would like to express their deep gratitude to Dr. David Lunn from the University of Leeds, UK, for sharing the experimental data that made this investigation possible.

7 References

[1] D.E. Lunn, E. De Pieri, G.J. Chapman, M.E. Lund, A.C. Redmond, S.J. Ferguson, Current Preclinical Testing of New Hip Arthroplasty Technologies Does Not Reflect Real-World Loadings: Capturing Patient-Specific and Activity-Related Variation in Hip Contact Forces, J. Arthroplasty. 35 (2020) 877–885. https://doi.org/10.1016/j.arth.2019.10.006.

[2] C. Fabry, S. Herrmann, M. Kaehler, E.-D. Klinkenberg, C. Woernle, R. Bader, Generation of physiological parameter sets for hip joint motions and loads during daily life activities for application in wear simulators of the artificial hip joint, Med. Eng. Phys. 35 (2013) 131–139. https://doi.org/10.1016/j.medengphy.2012.07.014.

[3] S.M. Kurtz, E. Lau, K. Ong, K. Zhao, M. Kelly, K.J. Bozic, Future Young Patient Demand for Primary and Revision Joint Replacement: National Projections from 2010 to 2030, Clin. Orthop. Relat. Res. 467 (2009) 2606–2612. https://doi.org/10.1007/s11999-009-0834-6.

[4] R. Viitala, V. Saikko, Effect of random variation of input and various daily activities on wear in a hip joint simulator, J. Biomech. 106 (2020) 109831. https://doi.org/10.1016/j.jbiomech.2020.109831.

[5] S. Affatato, F. Zanini, S. Carmignato, Quantification of Wear and Deformation in Different Configurations of Polyethylene Acetabular Cups Using Micro X-ray Computed Tomography, Materials. 10 (2017) 259. https://doi.org/10.3390/ma10030259.

[6] L. Mattei, F. Di Puccio, B. Piccigallo, E. Ciulli, Lubrication and wear modelling of artificial hip joints: A review, Tribol. Int. 44 (2011) 532–549. https://doi.org/10.1016/j.triboint.2010.06.010.

[7] L. Wang, G. Isaac, R. Wilcox, A. Jones, J. Thompson, Finite element analysis of polyethylene wear in total hip replacement: A literature review, Proc. Inst. Mech. Eng. [H]. 233 (2019) 1067–1088. https://doi.org/10.1177/0954411919872630.

[8] G. Bergmann, A. Bender, J. Dymke, G. Duda, P. Damm, Standardized Loads Acting in Hip Implants, PLOS ONE. 11 (2016) e0155612. https://doi.org/10.1371/journal.pone.0155612.

[9] G. Bergmann, G. Deuretzbacher, M. Heller, F. Graichen, A. Rohlmann, J. Strauss, G.N. Duda, Hip contact forces and gait patterns from routine activities, J. Biomech. 34 (2001) 859–871. https://doi.org/10.1016/s0021-9290(01)00040-9.

[10] L. Mattei, F. Di Puccio, E. Ciulli, A comparative study of wear laws for soft-on-hard hip implants using a mathematical wear model, Tribol. Int. 63 (2013) 66–77. https://doi.org/10.1016/j.triboint.2012.03.002.

[11] L. Mattei, F. Di Puccio, Wear Simulation of Metal-on-Metal Hip Replacements With Frictional Contact, J. Tribol. 135 (2013) 021402. https://doi.org/10.1115/1.4023207.

[12] G. Srivastava, N. Christian, C. Fred Higgs, A predictive framework of the tribological impact of physical activities on metal-on-plastic hip implants, Biotribology. 25 (2021) 100156. https://doi.org/10.1016/j.biotri.2020.100156.

[13] R. Nithyaprakash, S. Shankar, M.S. Uddin, Computational wear assessment of hard on hard hip implants subject to physically demanding tasks, Med. Biol. Eng. Comput. 56 (2018) 899–910. https://doi.org/10.1007/s11517-017-1739-2.

[14] V. Pakhaliuk, A. Poliakov, SIMULATION OF WEAR IN A SPHERICAL JOINT WITH A POLYMERIC COMPONENT OF THE TOTAL HIP REPLACEMENT CONSIDERING ACTIVITIES OF DAILY LIVING, Facta Univ. Ser. Mech. Eng. 16 (2018) 51–63. https://doi.org/10.22190/FUME171226006P.

[15] A. Ruggiero, A. Sicilia, S. Affatato, In silico total hip replacement wear testing in the framework of ISO 14242-3 accounting for mixed elasto-hydrodynamic lubrication effects, Wear. 460–461 (2020) 203420. https://doi.org/10.1016/j.wear.2020.203420.

[16] J.S.-S. Wu, J.-P. Hung, C.-S. Shu, J.-H. Chen, The computer simulation of wear behavior appearing in total hip prosthesis, Comput. Methods Programs Biomed. 70 (2003) 81–91. https://doi.org/10.1016/s0169-2607(01)00199-7.

[17] L. Mattei, F. Di Puccio, T.J. Joyce, E. Ciulli, Numerical and experimental investigations for the evaluation of the wear coefficient of reverse total shoulder prostheses, J. Mech. Behav. Biomed. Mater. 55 (2016) 53–66. https://doi.org/10.1016/j.jmbbm.2015.10.007.

[18] F. Di Puccio, L. Mattei, A novel approach to the estimation and application of the wear coefficient of metal-on-metal hip implants, Tribol. Int. 83 (2015) 69–76. https://doi.org/10.1016/j.triboint.2014.10.023.

[19] J.T. Weinhandl, H.J. Bennett, Musculoskeletal model choice influences hip joint load estimations during gait, J. Biomech. 91 (2019) 124–132. https://doi.org/10.1016/j.jbiomech.2019.05.015.

[20] E. De Pieri, M.E. Lund, A. Gopalakrishnan, K.P. Rasmussen, D.E. Lunn, S.J. Ferguson, Refining muscle geometry and wrapping in the TLEM 2 model for improved hip contact force prediction, PLOS ONE. 13 (2018) e0204109. https://doi.org/10.1371/journal.pone.0204109.

[21] X. Zhang, Z. Chen, L. Wang, W. Yang, D. Li, Z. Jin, Prediction of hip joint load and translation using musculoskeletal modelling with force-dependent kinematics and experimental validation, Proc. Inst. Mech. Eng. [H]. 229 (2015) 477–490. https://doi.org/10.1177/0954411915589115.

[22] D.E. Lunn, G.J. Chapman, A.C. Redmond, Hip kinematics and kinetics in total hip replacement patients stratified by age and functional capacity, J. Biomech. 87 (2019) 19–27. https://doi.org/10.1016/j.jbiomech.2019.02.002.
[23] D.E. Lunn, E. De Pieri, G.J. Chapman, M.E. Lund, A.C. Redmond, S.J. Ferguson, Current Preclinical Testing of New Hip Arthroplasty Technologies Does Not Reflect Real-World Loadings: Capturing Patient-Specific and Activity-Related Variation in Hip Contact Forces, J. Arthroplasty. 35 (2020) 877–885. https://doi.org/10.1016/j.arth.2019.10.006.
[24] LLJ – lifelongjoints.eu — Silicon Nitride Coatings for Improved Implant Function, (n.d.). https://lifelongjoints.eu/ (accessed July 21, 2021).
[25] D.L. Bartel, A.H. Burstein, M.D. Toda, D.L. Edwards, The Effect of Conformity and Plastic Thickness on Contact Stresses in Metal-Backed Plastic Implants, J. Biomech. Eng. 107 (1985) 193–199. https://doi.org/10.1115/1.3138543.
[26] S.L. Delp, F.C. Anderson, A.S. Arnold, P. Loan, A. Habib, C.T. John, E. Guendelman, D.G. Thelen, OpenSim: open-source software to create and analyze dynamic simulations of movement, IEEE Trans. Biomed. Eng. 54 (2007) 1940–1950. https://doi.org/10.1109/TBME.2007.901024.
[27] E. De Pieri, D.E. Lunn, G.J. Chapman, K.P. Rasmussen, S.J. Ferguson, A.C. Redmond, Patient characteristics affect hip contact forces during gait, Osteoarthritis Cartilage. 27 (2019) 895–905. https://doi.org/10.1016/j.joca.2019.01.016.
[28] F.C. Anderson, M.G. Pandy, Dynamic Optimization of Human Walking, J. Biomech. Eng. 123 (2001) 381–390. https://doi.org/10.1115/1.1392310.
[29] S.L. Delp, J.P. Loan, M.G. Hoy, F.E. Zajac, E.L. Topp, J.M. Rosen, An interactive graphics-based model of the lower extremity to study orthopaedic surgical procedures, IEEE Trans. Biomed. Eng. 37 (1990) 757–767. https://doi.org/10.1109/10.102791.
[30] How Inverse Kinematics Works - OpenSim Documentation - Global Site, (n.d.). https://simtk-confluence.stanford.edu:8443/display/OpenSim/How+Inverse+Kinematics+Works (accessed July 21, 2021).
[31] How RRA Works - OpenSim Documentation - Global Site, (n.d.). https://simtk-confluence.stanford.edu:8443/display/OpenSim/How+RRA+Works (accessed July 21, 2021).
[32] How CMC Works - OpenSim Documentation - Global Site, (n.d.). https://simtk-confluence.stanford.edu:8443/display/OpenSim/How+CMC+Works (accessed July 21, 2021).
[33] K.M. Steele, M.S. DeMers, M.H. Schwartz, S.L. Delp, Compressive tibiofemoral force during crouch gait, Gait Posture. 35 (2012) 556–560. https://doi.org/10.1016/j.gaitpost.2011.11.023.
[34] F. Di Puccio, L. Mattei, In-silico analytical wear predictions: application to joint prostheses (In Press), in: Wear Adv. Eng. Appl. Mater., Rodríguez-Tembleque, Luis Vázquez, Jesús Aliabadi, M H Ferri, n.d.
[35] T.A. Maxian, T.D. Brown, D.R. Pedersen, J.J. Callaghan, A sliding-distance-coupled finite element formulation for polyethylene wear in total hip arthroplasty, J. Biomech. 29 (1996) 687–692. https://doi.org/10.1016/0021-9290(95)00125-5.
[36] L.A. Vogel, G. Carotenuto, J.J. Basti, W.N. Levine, Physical Activity After Total Joint Arthroplasty, Sports Health Multidiscip. Approach. 3 (2011) 441–450. https://doi.org/10.1177/1941738111415826.
[37] M. Morlock, E. Schneider, A. Bluhm, M. Vollmer, G. Bergmann, V. Müller, M. Honl, Duration and frequency of every day activities in total hip patients, J. Biomech. 34 (2001) 873–881. https://doi.org/10.1016/S0021-9290(01)00035-5.
[38] J.T. Weinhandl, B.S. Irmischer, Z.A. Sievert, Effects of Gait Speed of Femoroacetabular Joint Forces, Appl. Bionics Biomech. 2017 (2017) e6432969. https://doi.org/10.1155/2017/6432969.
[39] A. Cappozzo, F. Catani, A. Leardini, M. Benedetti, U. Della Croce, Position and orientation in space of bones during movement: experimental artefacts, Clin. Biomech. 11 (1996) 90–100. https://doi.org/10.1016/0268-0033(95)00046-1.
[40] V. Carbone, M.M. van der Krogt, H.F.J.M. Koopman, N. Verdonschot, Sensitivity of subject-specific models to errors in musculo-skeletal geometry, J. Biomech. 45 (2012) 2476–2480. https://doi.org/10.1016/j.jbiomech.2012.06.026.
[41] L. Bosmans, G. Valente, M. Wesseling, A. Van Campen, F. De Groote, J. De Schutter, I. Jonkers, Sensitivity of predicted muscle forces during gait to anatomical variability in musculotendon geometry, J. Biomech. 48 (2015) 2116–2123. https://doi.org/10.1016/j.jbiomech.2015.02.052.
[42] M. Wesseling, F.D. Groote, L. Bosmans, W. Bartels, C. Meyer, K. Desloovere, I. Jonkers, Subject-specific geometrical detail rather than cost function formulation affects hip loading calculation, Comput. Methods Biomech. Biomed. Engin. 19 (2016) 1475–1488. https://doi.org/10.1080/10255842.2016.1154547.
[43] L. Kang, A.L. Galvin, T.D. Brown, J. Fisher, Z.-M. Jin, Wear simulation of ultra-high molecular weight polyethylene hip implants by incorporating the effects of cross-shear and contact pressure, Proc. Inst. Mech. Eng. [H]. 222 (2008) 1049–1064. https://doi.org/10.1243/09544119JEIM431.

[44] L. Kang, A.L. Galvin, J. Fisher, Z. Jin, Enhanced computational prediction of polyethylene wear in hip joints by incorporating cross-shear and contact pressure in additional to load and sliding distance: Effect of head diameter, J. Biomech. 42 (2009) 912–918. https://doi.org/10.1016/j.jbiomech.2009.01.005.
[45] F. Liu, A. Galvin, Z. Jin, J. Fisher, A New Formulation for the Prediction of Polyethylene Wear in Artificial Hip Joints, Proc. Inst. Mech. Eng. [H]. 225 (2011) 16–24. https://doi.org/10.1243/09544119JEIM819.
[46] C. Kaddick, M.A. Wimmer, Hip simulator wear testing according to the newly introduced standard ISO 14242, Proc. Inst. Mech. Eng. [H]. 215 (2001) 429–442. https://doi.org/10.1243/0954411011536019.
[47] M. Ali, M. Al-Hajjar, S. Partridge, S. Williams, J. Fisher, L.M. Jennings, Influence of hip joint simulator design and mechanics on the wear and creep of metal-on-polyethylene bearings, Proc. Inst. Mech. Eng. [H]. 230 (2016) 389–397. https://doi.org/10.1177/0954411915620454.
[48] G. Matsoukas, R. Willing, I.Y. Kim, Total Hip Wear Assessment: A Comparison Between Computational and In Vitro Wear Assessment Techniques Using ISO 14242 Loading and Kinematics, J. Biomech. Eng. 131 (2009) 041011. https://doi.org/10.1115/1.3049477.